

## Theory of a symmetry-breaking phase transition in a surface layer of nematic liquid crystal

Y. L'vov and R. M. Hornreich

*Department of Electronics, Weizmann Institute of Science, 76100 Rehovot, Israel*

D. W. Allender

*Department of Physics and Liquid Crystal Institute, Kent State University, Kent, Ohio 44242*

(Received 11 December 1992)

For a surface interaction linear in the order parameter and favoring an orientation in which liquid-crystalline molecules lie parallel to the surface (but which is independent of whether the orientation is uniaxial or isotropic in the bounding plane), a symmetry-breaking phase transition in a surface layer is possible at temperatures above that of the bulk isotropic to nematic transition. At the surface transition, the high-temperature in-plane isotropic state becomes unstable with respect to a biaxial phase, the transition being continuous and therefore of the Berezinskii-Kosterlitz-Thouless (BKT) type. It is expected to occur for intermediate surface couplings but not at very weak or very strong couplings. The bulk phase always remains disordered. The BKT transition boundary is calculated explicitly and the results are compared with earlier theoretical studies on systems with linear or quadratic surface interaction potentials. Numerical estimates indicate that systems having the required linear surface potentials can be prepared and possible techniques for observing a BKT-type phase transition are discussed.

PACS number(s): 61.30.Gd, 64.70.Md, 68.45.-v

### I. INTRODUCTION

It is well known that rodlike nematic liquid-crystal systems undergo a (first-order) phase transition from an isotropic to a uniaxially ordered state at a critical temperature  $T_c$ . However, while no *bulk* ordering occurs when  $T > T_c$ , there will be local ordering in the vicinity of the bounding surface whenever there exists a surface potential preferentially orienting the liquid-crystal molecules [1–8]. Such ordering, of course, decays rapidly with distance from the boundary.

The simplest types of surface interactions are those orienting the molecules preferentially either in or normal to the boundary. There are then three possibilities: One, the preferred orientation is along the normal; two, the preferred molecular orientation is along a unique axis lying in the bounding surface; three, there is no unique axis in the surface but the molecules lie preferentially in this plane.

For the first two possibilities, Sheng [1,4] and, later, Mauger *et al.* [6] pointed out that there were *two* possible ordered surface states, both having the same symmetry. Alternately, these two states can be regarded as “thin” and “thick” layer phases, which are separated by a prewetting transition. In fact, the phase diagram in [6] was first presented from this point of view by Nakanishi and Fisher [9]. The prewetting transition line in the interaction-strength–temperature plane separating the two states terminates in a critical point and much of the subsequent literature in this area [5,7,8] uses this description. A review can be found in [10].

The third possibility (i.e., preferential planar orientation) was initially studied by Sluckin and Poniewierski [7]. They pointed out that this boundary condition allows surface ordered states with different symmetries to

exist and that there can then be spontaneous phase transitions between them. In particular, these authors considered an interaction potential linearly proportional to the ordering at the surface and solved the resulting differential equations in a limiting case (in which one of the two symmetry-allowed elastic constants vanishes). They indeed found that transitions between distinct, thermodynamically stable, ordered states could occur and noted that, when continuous, these transitions could be characterized by Berezinskii-Kosterlitz-Thouless (BKT) [11,12] critical behavior.

In this work, we reconsider the Landau–de Gennes free energy expression of Sluckin and Poniewierski and obtain solutions for general values of the elastic constants. The resulting phase diagrams have features in common with that given in [7] but differ in some aspects. We do find, in agreement with [7], a continuous phase boundary, which we also calculate via the BKT approach.

In the final section, we compare our results with those given in the literature [7,13] and comment on the similarities and differences. In addition, the possibility of observing the predicted phase boundaries experimentally is discussed.

### II. THE SURFACE-INDUCED PHASE TRANSITION BOUNDARY

#### A. Uniaxial phases

Consider a nematic liquid crystal confined to the half space  $z > 0$ . The appropriate Landau–de Gennes bulk free energy is [14]

$$F_b = \int d^3r \left[ \frac{1}{2}(a\epsilon_{ij}^2 + c_1\epsilon_{ij,l}^2 + c_2\epsilon_{ij,i}\epsilon_{ij,l}) - \beta\epsilon_{ij}\epsilon_{jl}\epsilon_{li} + \gamma(\epsilon_{ij}^2)^2 \right], \quad (1a)$$

where  $\epsilon_{ij}$  is the anisotropic (traceless) part of the dielectric constant,  $a$  is proportional to a reduced temperature,  $c_1$ ,  $c_2$ ,  $\beta$ , and  $\gamma$  are temperature-independent constants,  $\epsilon_{ij,l} \equiv \partial\epsilon_{ij}/\partial x_l$ , and we sum on repeated indices. The indices  $(i, j, l)$  run from 1 to 3.

We simplify our notation by setting

$$\begin{aligned} \epsilon_{ij} &= s\mu_{ij}, \quad s = \beta/\sqrt{6}\gamma, \quad f = F/(\beta^4/36\gamma^3), \\ \frac{1}{4}t &= (3\gamma/\beta^2)a, \quad \frac{1}{4}\xi^2 = (3\gamma/\beta^2)c_1, \quad \rho = c_2/c_1. \end{aligned} \quad (1b)$$

Then Eq. (1a) becomes

$$f_b = \int d^3r \left\{ \frac{1}{4}[t\mu_{ij}^2 + \xi^2(\mu_{ij,l}^2 + \rho\mu_{ij,i}\mu_{ij,l})] - \sqrt{6}\mu_{ij}\mu_{jl}\mu_{li} + (\mu_{ij}^2)^2 \right\}. \quad (1c)$$

For a uniaxial system uniform in the  $x$ - $y$  plane and having  $z$  as one of its principal axes, the reduced tensor order parameter  $\mu_{ij}$  can always be written either as

$$\mu_{ij} = \frac{1}{\sqrt{6}}\mu_1(\xi) \begin{pmatrix} 2 & 0 & 0 \\ 0 & -1 & 0 \\ 0 & 0 & -1 \end{pmatrix} (U_1), \quad (2a)$$

or

$$\mu_{ij} = \frac{1}{\sqrt{6}}\mu_2(\xi) \begin{pmatrix} -1 & 0 & 0 \\ 0 & -1 & 0 \\ 0 & 0 & 2 \end{pmatrix} (U_2), \quad (2b)$$

with  $\xi = z/\xi$  a normalized  $z$  coordinate [14]. For  $U_1$ , the unique direction is in the surface plane while for  $U_2$  it is normal to the surface. Substituting Eqs. (2) into Eq. (1c) and defining  $A$  as the area in the  $x$ - $y$  plane, the normalized bulk free energy becomes

$$\frac{f_b}{A\xi} = \int d\xi \left[ \frac{1}{4}t\mu_i^2 - \mu_i^3 + \mu_i^4 + \frac{1}{4} \left( \frac{d\mu_i}{d\xi} \right)^2 \right] \quad (\iota = 1, 2). \quad (3a)$$

Here  $\Gamma_1 = \xi/(1 + \rho/6)^{1/2} = \xi/\omega_1$  and  $\Gamma_2 = \xi/(1 + 2\rho/3)^{1/2} = \xi/\omega_2$ . The index values  $\iota = 1, 2$  relate to  $U_1$  and  $U_2$ , respectively.

We now supplement  $f_b$  with a surface term which models, to lowest order in the nematic order parameter, the torques acting on the molecules at the surface. As noted, we are specifically interested in the case wherein these torques favor an in-plane molecular orientation. Following Sluckin and Poniewierski [7], we therefore take

$$\begin{aligned} f_s/A\xi &= \int d\xi \tilde{\nu}(\mu_{33})\delta(\xi) \\ &= \alpha_\iota \nu \mu_\iota(0) = \begin{cases} -\frac{1}{2}\nu\mu_1(0) & (U_1) \\ \nu\mu_2(0) & (U_2) \end{cases}, \end{aligned} \quad (3b)$$

with  $\nu = \sqrt{2/3}\tilde{\nu}$ , which is proportional to the pinning torque at the surface, positive.

Before proceeding, the following points should be noted: The factor of  $(-2)$  in Eq. (3b) differentiating between the two possible surface configurations is connected to the order parameter normalization chosen in Eqs. (2). By setting  $\mu_2(\xi) = -\tilde{\mu}_2(\xi)/2$ , for example, we could make  $f_s$  formally identical for the two cases. In fact, this is the more transparent choice since, physically, the surface potential energy is always minimized when the molecules lie in the plane. Using  $\tilde{\mu}_2$ , the surface energy term would be identical for both cases as the magnitudes of the components of the respective order parameters normal to the surface are then equal. Our normalization, however, is more convenient mathematically as the expressions for the bulk free energy are then formally identical. The final result, of course, is independent of the choice of order parameter normalization.

In order for the surface energy  $f_s$  to make the total system free energy negative above  $T_c$  (i.e., for  $t > 1$ ), it is necessary that  $\mu_2(0)$  be negative. (The bulk energy  $f_b$  is, of course, always positive for  $t > 1$ .) On the other hand, this negative amplitude increases  $f_b$  (via the cubic term). It is this competition between the surface and bulk contributions to the total free energy which makes possible a phase transition between surface states when  $t > 1$ .

Minimizing the total free energy  $f = f_b + f_s$  yields a variational equation for  $\mu_\iota$  whose first integral is

$$\frac{1}{4} \left( \frac{d\mu}{d\xi} \right)^2 = \frac{1}{4}t\mu^2 - \mu^3 + \mu^4. \quad (4)$$

For clarity, we have suppressed the  $\iota$  subscripts on  $\mu$  and  $\xi$ . Integrating Eq. (4) gives

$$\mu = \frac{\frac{1}{2}t}{1 + \sqrt{t-1} \sinh(\pm\sqrt{t}\xi/\Gamma + \psi_0)}, \quad (5)$$

where the upper and lower signs refer to  $\iota = 1, 2$ , respectively, and the phase  $\psi_0$  (whose  $\iota$  subscript has also been suppressed) is directly related to  $\mu(\xi = \Gamma = 0) = \mu_0$ .

From Eqs. (3a) and (4), it is clear that

$$\frac{f_b}{A\xi} = \frac{1}{2} \int_0^\infty d\xi \left( \frac{d\mu}{d\xi} \right)^2 = \frac{1}{2}\omega \int_0^\infty d\xi \left( \frac{d\mu}{d\xi} \right)^2, \quad (6)$$

where we have again suppressed the subscripts (on  $\mu$ ,  $\omega$ , and  $\xi$ ). Using Eq. (5), we obtain

$$\begin{aligned} \frac{f_b}{A\xi} &= \frac{\omega}{24} \left\{ [4\mu_0^2 - \mu_0 + \frac{1}{2}(2t-3)](4\mu_0^2 - 4\mu_0 + t)^{1/2} - \frac{1}{2}\sqrt{t}(2t-3) \right. \\ &\quad \left. + 3(t-1) \left[ \operatorname{arctanh} \left( \frac{1 \mp \sqrt{t-1}}{\sqrt{t}} \right) \mp \operatorname{arctanh} \left( \frac{\tanh(\psi_0/2) - \sqrt{t-1}}{\sqrt{t}} \right) \right] \right\}. \end{aligned} \quad (7a)$$

The surface free energy  $f_s$  is given in terms of  $\mu_0$  by Eq. (3b). Alternately, it can be written as

$$\frac{f_s}{A\xi} = -\frac{\omega}{24}(24\mu_0^2)(4\mu_0^2 - 4\mu_0 + t)^{1/2}. \quad (7b)$$

Thus we need only determine  $\mu_0$  as a function of  $\nu$  and  $t$ . This is done by integrating the variational equation for  $\mu$  through an infinitesimal interval about  $\zeta=0$  [15]. The result is

$$\left( \frac{d\mu}{d\Gamma} \right)_0 = \frac{\alpha\nu}{\omega}, \quad (8)$$

where [see Eq. (3)]  $\alpha_1 = -\frac{1}{2}$ ,  $\alpha_2 = 1$ , and the derivative is evaluated at  $\zeta=0$ . Using Eq. (4), Eq. (8) yields the quartic equation

$$\mu_0^4 - \mu_0^3 + \frac{t}{4}\mu_0^2 - \frac{\alpha^2\nu^2}{4\omega^2} = 0, \quad (9)$$

whose solution gives the appropriate values of  $\mu_0$  for  $U_1$  and  $U_2$ , respectively.

For  $U_1$  (in-plane uniaxial state),  $\mu_0 = \mu_1(0) > 0$  and Eq. (9) has either one or three real and positive solutions. The single solution is always locally stable; when there are three solutions, two are locally stable. For the latter case, there is a "shelf" in the  $(t, \nu, \rho)$  parameter space which defines the thermodynamic boundary between the two stable solutions. This is a prewetting transition line. (Mauger *et al.* [6] referred to it as the boundary between "weak" and "strong" surface states.) This shelf is bounded, at  $t=1$ , by the line  $\nu = (2\sqrt{3}-3)^{1/2}(1+\rho/6)^{1/2}/8$  and, at  $t = \frac{9}{8}$ , by the line of critical points  $\nu = 3\sqrt{3}(1+\rho)^{1/2}/32$ . Above the shelf, the thick or "strong" state is energetically preferred, below it, the thin or "weak" one. For  $t > \frac{9}{8}$ , the two states are indistinguishable.

For  $U_2$  (in-plane isotropic state),  $\mu_0 = \mu_2(0) < 0$  and Eq. (9) has only a single real and negative (and stable) solution. Thus, for the case of uniaxial surface states, our analysis reduces to (a) calculating, for given  $(t, \nu, \rho)$ ,  $\mu_1(0)$ , and  $\mu_2(0)$ , [for  $1 < t < \frac{9}{8}$ , the  $\mu_1(0)$  solution giving the lower free energy is chosen], (b) using Eqs. (7) to obtain  $f = f_b + f_s$  for both cases, and (c) finding the phase boundary separating the regions in the parameter space where  $f_1 < f_2$  and vice versa. On the  $f_1 = f_2$  boundary, there is a first-order phase transition between the two uniaxial surface states.

The above procedure was carried out numerically; the results are summarized in Fig. 1. We see that there indeed exists a region in the phase diagram in which the in-plane uniaxial surface state is thermodynamically stable. This region is bounded, for fixed  $\rho$ , by the  $t=1$  boundary at which the bulk transition occurs and by a closed curve intersecting the  $t=1$  line at the minimal and maximal values of  $\nu$  for which the in-plane uniaxial phase is stable. The curve reaches its maximum  $\nu$  value at an intermediate value of  $\nu$ . Of course, these  $\nu$  values are all  $\rho$  dependent.

We also find that the first-order phase boundary lies, for all physically relevant values of  $\rho$  and  $1 < t < \frac{9}{8}$ , above

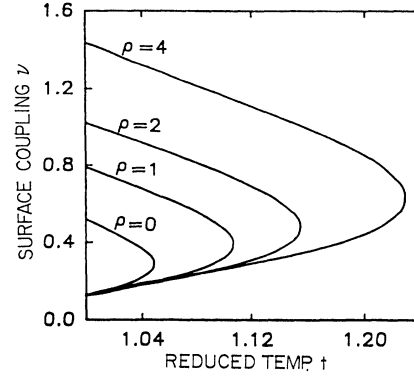


FIG. 1. Phase boundary in the (temperature)-(surface potential amplitude)  $(t-\nu)$  plane between uniaxially ordered surface states with the unique axis parallel (in-plane uniaxial phase—to the left of the curves) and normal (in-plane isotropic phase) to the plane of the boundary. Shown are theoretical boundaries for different values of the Landau elastic constant ratio  $\rho$ . The bulk phase is disordered for  $t > 1$ .

the prewetting transition or "weak-strong shelf." That is, the transition from the in-plane isotropic to in-plane uniaxial state always results in the latter being in the so-called thick or "strong" state or, in other words, the prewetting transition is preempted. For this reason, this prewetting line is not shown in the figure.

## B. The biaxial phase

The analysis given in Sec. II A and summarized graphically in Fig. 1, while exact, is restricted since only states characterized by uniaxial ordering were allowed. We now relax this restriction in order to study possible biaxial surface ordering. Indeed, a solution of this type was found by Sluckin and Poniewierski [7] (whose analysis, in our notation, corresponds to the regime  $\rho \rightarrow \infty$ ).

The general biaxial case can be studied by considering a tensor order parameter having the form

$$\mu_{ij} = \frac{1}{\sqrt{6}} \begin{pmatrix} 2\mu_1 & 0 & 0 \\ 0 & -\mu_1 - \eta_1 & 0 \\ 0 & 0 & -\mu_1 + \eta_1 \end{pmatrix} (B_1). \quad (10a)$$

For  $|\eta_1(\xi)| \ll |\mu_1(\xi)|$  this can be regarded as a perturbation on the  $U_1$  uniaxial order parameter given in Eq. (2a). Of course, one could equally consider the alternate formulation [see Eq. (2b)]

$$\mu_{ij} = \frac{1}{\sqrt{6}} \begin{pmatrix} -\mu_2 + \eta_2 & 0 & 0 \\ 0 & -\mu_2 - \eta_2 & 0 \\ 0 & 0 & 2\mu_2 \end{pmatrix} (B_2). \quad (10b)$$

For unrestricted values of  $\mu_i$  and  $\eta_i$  ( $i=1,2$ ), these two formulations are equivalent. However, it will be con-

venient to use these alternate forms whenever the  $\eta_i$  are considered as perturbations of the respective uniaxial solutions found in Sec. II A.

The alternate order parameters given above yield different expressions for the total free energy  $f = f_b + f_s$  of a biaxial phase. Thus, using Eq. (10a), we obtain

$$\frac{f_b}{A\xi} = \int d\xi \left[ \frac{1}{4}t\mu_1^2 + \frac{1}{12}t\eta_1^2 - \mu_1^3 + \mu_1\eta_1^2 + \mu_1^4 + \frac{2}{3}\mu_1^2\eta_1^2 + \frac{1}{9}\eta_1^4 + \frac{\omega_1^2}{4}(\mu_1')^2 + \frac{1}{12} \left[ 1 + \frac{\rho}{2} \right] (\eta_1')^2 - \frac{\rho}{12}\mu_1'\eta_1' \right], \quad (11a)$$

$$f_s / A\xi = -\frac{1}{2}v[\mu_1(0) - \eta_1(0)], \quad (11b)$$

while the alternative, Eq. (10b), gives

$$\frac{f_b}{A\xi} = \int d\xi \left[ \frac{1}{4}t\mu_2^2 + \frac{1}{12}t\eta_2^2 - \mu_2^3 + \mu_2\eta_2^2 + \mu_2^4 + \frac{2}{3}\mu_2^2\eta_2^2 + \frac{1}{9}\eta_2^4 + \frac{\omega_2^2}{4}(\mu_2')^2 + \frac{1}{12}(\eta_2')^2 \right], \quad (12a)$$

$$f_s / A\xi = v\mu_2(0). \quad (12b)$$

The prime in these equations denotes differentiation with respect to  $\xi$ .

Minimizing the total energy  $f$  yields, for either choice of biaxial order parameter, two coupled nonlinear differential equations, with no apparent analytic solution. We choose, therefore, to use a method giving an *upper bound* on the true ground-state energy for given  $(t, v, \rho)$ . Our approach (known as a Ritz procedure) was to (a) substitute, in Eq. (11) or (12), the function  $\mu_i(\xi)$  ( $i=1, 2$ , respectively), given in Eq. (5) [i.e., the exact solutions for  $\eta_i(\xi)=0$ ] and (b) use a trial function for  $\eta_i(\xi)$ . Incorporated in the latter are a small number (we choose two) of parameters which are ultimately fixed by the minimization of the free energy.

Our choice of trial functions  $\eta_i(\xi)$  was governed by two considerations: (1) they must vanish as  $\xi \rightarrow \infty$ , and (2) they should permit an analytic evaluation of the integrals in  $f_b$ . The latter, of course, is for convenience of calculation while the former is an absolute requirement. Our choice was

$$\eta(\xi) = \frac{\frac{1}{2}at}{1 + b \sinh[\pm\sqrt{t}\xi/\omega + \psi_0]}, \quad (13)$$

where, as in Eq. (5), the  $\iota$  subscripts (here on  $\eta$ ,  $\omega$ ,  $\psi_0$ ,  $a$ , and  $b$ ) have been suppressed.

Consider first  $B_1$ . Since there are terms in  $f$  [see Eq. (11)] which are *linear* in  $\eta_1$  (and its derivative), it follows that  $U_1$  is *always* unstable with respect to biaxiality. Thus the  $U_1$  region in the phase diagram of Fig. 1 will be *entirely replaced by one with biaxial order* once the uniaxial order parameter constraint is relaxed.

For  $B_2$ , on the other hand, there are *no* contributions to  $f$  linear in  $\eta_2$  or its derivatives. Thus the  $U_2$  uniaxial

phase *can* be stable and it follows that a continuous (second-order transition) between  $U_2$  and a biaxially ordered phase is, in principle, possible.

Quantitative verification of these general observations was obtained by substituting Eqs. (5) and (13) into Eqs. (11) and (12), respectively, and calculating analytically the energy functionals  $f(B_1; [a, b])$  and  $f(B_2; [a, b])$ . For  $B_2$ , the boundary condition is unchanged from the  $U_2$  uniaxial case [see Eq. (12b)] and is  $[a, b]$  independent while, for  $B_1$ , there is an additional contribution proportional to  $\eta_1(0)$  [see Eq. (11b)]. The latter is  $[a, b]$  dependent and was included in  $f(B_1; [a, b])$ . The two free energy functionals were then minimized numerically with respect to the parameters  $[a, b]$  at points in the  $(t-v)$  phase diagram for fixed elastic constant ratio  $\rho$ . The re-

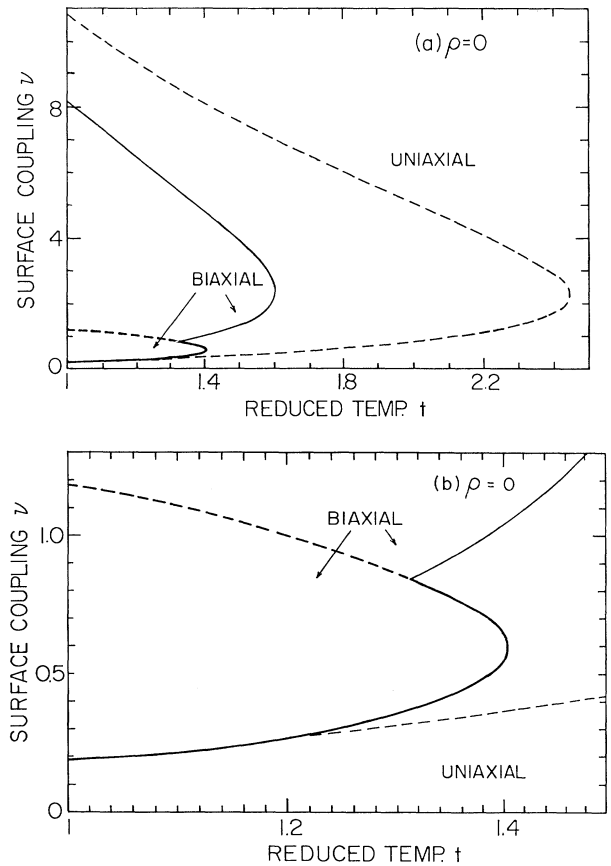


FIG. 2. Landau theory phase boundaries in the (temperature)-(surface potential amplitude)  $(t-v)$  plane between surface states with different ordering for the elastic constant ratio  $\rho=0$ . Shown are a high-temperature in-plane isotropic uniaxially ordered phase and a biaxial phase. The latter is divided into two regions having the same symmetry but separated by a first-order phase boundary (denoted by a heavy broken line). The lower part (shown as a heavy full line) of the boundary between the uniaxial and biaxial phases is first order while the upper part (light broken line) is continuous. Also shown (light full line) is the Berezinskii-Kosterlitz-Thouless transition boundary, which is the relevant one for two-dimensional systems. (b) is an enlargement of the lower-left-hand section of (a).

sulting free energy values were then compared with each other and with those of the uniaxial phases  $U_1, U_2$ . The results, for  $\rho=0, 1$ , and  $10$ , are summarized graphically in Figs. 2–4.

As expected, we find that the  $U_1$  phase (see Fig. 1) no longer appears—it is replaced by a biaxial one. However,  $U_2$  does remain stable in a region of the phase diagram and there is either a second-order transition boundary between it and the  $B_2$  biaxial phase or (for small  $\nu$ ) a first-order transition between it and the  $B_1$  biaxial phase.

We also find a discontinuous (first-order or prewetting) transition boundary between the  $B_1$  and  $B_2$  regions. However, this result must be regarded cautiously: These phases have the same symmetry and thus, in principle, the phase boundary between them could terminate in a critical point (analogous to that found in liquid-gas phase diagrams or for the case of a positive dielectric anisotropy nematic liquid crystal in an external field [10]). Given the nature of the approximation we are using (wherein  $B_1$  and  $B_2$  are obtained by adding biaxial trial functions to the uniaxial solutions  $U_1$  and  $U_2$ , respectively), such a critical point, if it indeed exists, would not be found. We shall return to this point in Sec. III.

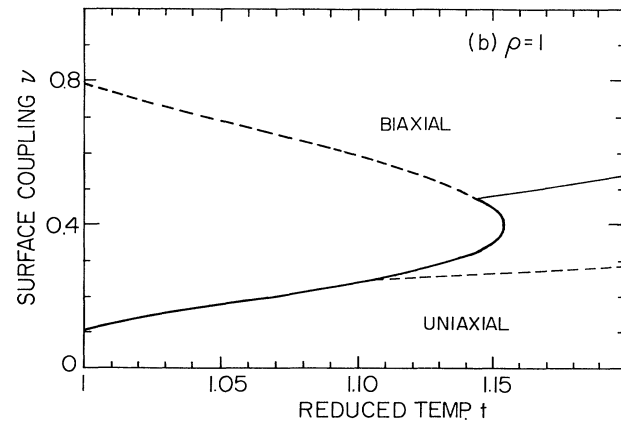
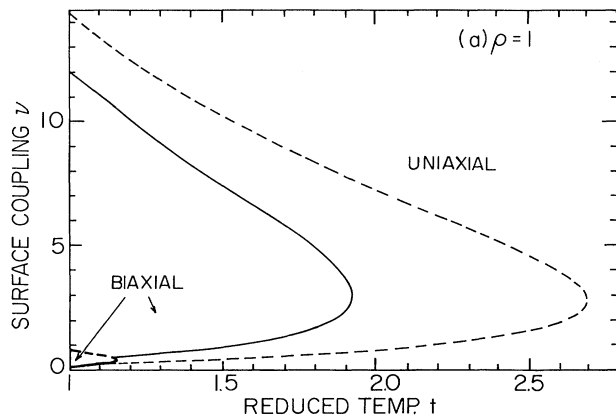


FIG. 3. Phase boundaries in the (temperature)-(surface potential amplitude) ( $t$ - $\nu$ ) plane between surface states with different ordering for the elastic constant ratio  $\rho=1$ . Other details as in Fig. 2.

### C. The Berezinskii-Kosterlitz-Thouless phase transition

In Sec. II B, we found, via Landau theory, a continuous phase boundary between a uniaxial surface state and a biaxial one in a region of the (temperature)-(surface interaction potential magnitude) ( $t$ - $\nu$ ) phase diagram. However, since this transition is between surface ordered states, it is fundamentally two dimensional in character and fluctuation effects are therefore of central importance.

As shown by BKT [11,12], the fluctuations relevant to continuous phase transitions in two-dimensional systems are long-wavelength in-plane phase distortions of the relevant order parameter. For nematic liquid crystals, these are associated with free energy terms of the form [12,16]

$$F_{\text{BKT}} = \frac{1}{2}K \int d^2r (\nabla\theta)^2, \quad (14)$$

where  $\theta = \theta(x, y)$  is the fluctuating in-plane angle between a local in-plane principal axis and a fixed reference axis and  $K$  is a stiffness (elastic) constant.

In our case, we have an ordered layer of finite thickness rather than a true two-dimensional system. However, near the transition boundary, the layer may be regarded

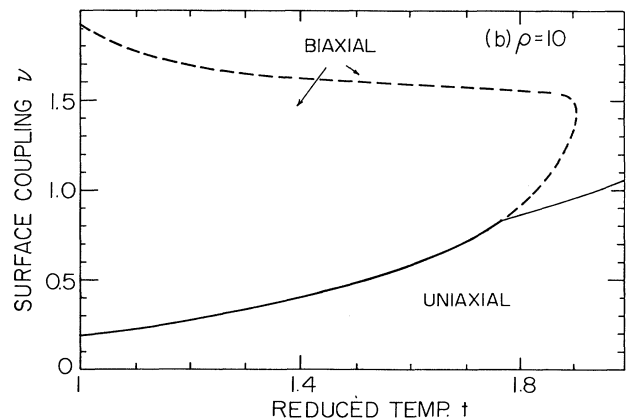
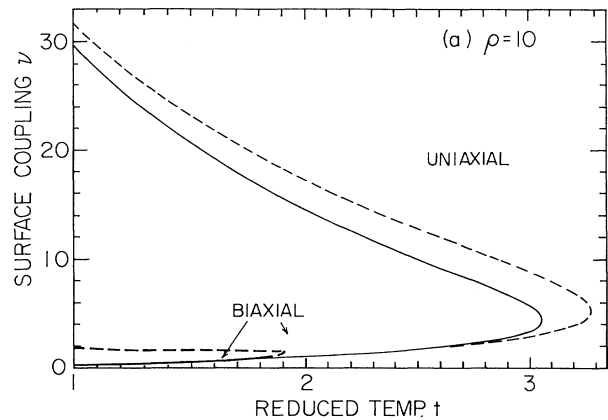


FIG. 4. Phase boundaries in the (temperature)-(surface potential amplitude) ( $t$ - $\nu$ ) plane between surface states with different ordering for the elastic constant ratio  $\rho=10$ . Other details as in Fig. 2.

as effectively two dimensional, with the relevant fluctuations characterized by an effective stiffness  $K_b$  which is connected with the bulk free energy coefficients  $\beta$  and  $\gamma$  and the elastic moduli  $c_1, c_2$ . To see this, we return to Eq. (1c) and note that fluctuations contribute to  $f_b$  via the terms

$$\begin{aligned} F_{\text{elastic}} &= \left[ \frac{\beta^4}{36\gamma^3} \right] f_{\text{elastic}} \\ &= \left[ \frac{c_1\beta^2}{12\gamma^2} \right] \int d^3r (\mu_{ij,l}^2 + \rho\mu_{ij,i}\mu_{ij,l}). \end{aligned} \quad (15a)$$

For the case of the continuous phase transition between  $U_2$  and  $B_2$ , the symmetry-breaking order parameter is the biaxial component  $\eta_2$  of  $\mu_{ij}$  [see Eq. (10b)]. The part of  $\mu_{ij}$  relevant to in-plane angular (i.e., phase) fluctuations can then be written as [13,16]

$$[\mu_{ij}]_{\text{fluc}} = \frac{1}{\sqrt{6}} \eta_2(\xi) \begin{bmatrix} \cos 2\theta & \sin 2\theta \\ \sin 2\theta & -\cos 2\theta \end{bmatrix}. \quad (15b)$$

$$\begin{aligned} k_B T_S &= \frac{\pi\sqrt{3}}{72} \left[ \frac{c_1}{\gamma} \right]^{3/2} \beta a^2 t_S^{3/2} \left[ 1 + \frac{\rho}{2} \right] \left[ 1 + \frac{2\rho}{3} \right]^{1/2} (1+b^2)^{-1} \\ &\times \left\{ -1 - \frac{b \cosh \psi_0}{1+b \sinh \psi_0} + \frac{2}{\sqrt{1+b^2}} \left[ \operatorname{arctanh} \left( \frac{1+b}{\sqrt{1+b^2}} \right) + \operatorname{arctanh} \left( \frac{\tanh(\psi_0/2) - b}{\sqrt{1+b^2}} \right) \right] \right\}. \end{aligned} \quad (18)$$

In order to evaluate  $t_s$  in Eq. (18), we require representative values for the parameters  $\beta$ ,  $\gamma$ ,  $c_1$ , and  $\rho$ . These will be introduced in the following section, where we also calculate the BKT transition boundary.

### III. DISCUSSION

In the preceding section, we showed that, under specified boundary conditions, a new type of phase transition can occur in an ordered surface layer even though the bulk nematic system is disordered. Here, we introduce representative values for the system parameters, calculate the BKT transition boundary, compare our results with those in the literature, and consider possible ways of observing the predicted transition experimentally.

In order to obtain physical values for the parameters in the free energy, we make use of the standard expression [4]

$$F = \int dz [AS^2 - BS^3 + DS^4 + L(dS/dz)^2 + \alpha_1 GS\delta(z)]. \quad (19)$$

Comparing this expression with Eqs. (2) and (3), we set  $\mu = SD/B$ ,  $\xi = Bz/2\sqrt{LD}$ ,  $\nu = D^{3/2}G/2\sqrt{L}B^2$ , and  $f = D^{5/2}F/2\sqrt{L}B^3$ . Taking as typical values [4,17]  $B = \beta/\sqrt{6} = 0.53 \times 10^7$  ergs/cm<sup>3</sup>,  $D = \gamma = 0.98 \times 10^7$  ergs/cm<sup>3</sup>, and  $L = \frac{1}{2}c_1 = 4.5 \times 10^{-7}$  ergs/cm, we obtain

Substituting Eq. (15b) into Eq. (15a) and comparing with Eq. (14) gives

$$\begin{aligned} F_{\text{BKT}} &= \frac{1}{2} K_b \int d^2r (\nabla\theta)^2 \\ &= \frac{1}{2} \left[ \left( \frac{2\beta^2}{9\gamma^2} \right) (c_1\xi) \left[ 1 + \frac{\rho}{2} \right] \int_{0^+}^{\infty} d\xi \eta_2^2(\xi) \right] \\ &\quad \times \int d^2r (\nabla\theta)^2. \end{aligned} \quad (16)$$

Since there is no purely two-dimensional system in addition to the ordered surface layer, the critical temperature of the BKT phase transition is given by [16]

$$\lim_{T \rightarrow T_s^-} K_b = \frac{8}{\pi} k_B T_S, \quad (17)$$

where  $k_B$  is Boltzmann's constant. Using Eqs. (13) and (16), we then have

$$G = 2\sqrt{L}B^2\nu/D^{3/2} = 1.2\nu \text{ ergs/cm}^2. \quad (20)$$

Thus  $\nu=1.0$  is equivalent to  $G=1.2$  ergs/cm<sup>2</sup>. This value of  $G$ , which is in the theoretically interesting range, can be compared with experimental determinations of  $G$ , or with measurements of anchoring energy,  $W$ , by means of the relationship  $W \approx 3G|S(0)|$ . From an analysis of birefringence data on 4-cyano-4'-n-pentabiphenyl (5CB), Yokoyama [18,19] reported  $G \sim 38$  ergs/cm<sup>2</sup> for a rubbed polyvinyl alcohol coated surface, but only 0.85 erg/cm<sup>2</sup> for a SiO film on the substrate. Furthermore, a review of measurements of anchoring energies [20] notes that values of  $W$  range from 1 down to  $10^{-4}$  erg/cm<sup>2</sup>. Thus it is expected that surfaces with appropriate interaction potentials to test the predicted phase transition can be prepared.

Assuming that the required conditions on the surface potential can be met, the reduced BKT transition temperature  $t_s$  between the high-temperature uniaxial phase  $U_2$  and the biaxial phase  $B_2$  can be calculated using the representative parameters given above and Eq. (18) and taking  $T_c \approx T_S \approx 350$  K. The results, for  $\rho=0, 1$ , and  $10$ , respectively, are given in Figs. 2-4. As expected, we see that the biaxially ordered phase becomes unstable with respect to long-wavelength in-plane fluctuations before (i.e., at a lower temperature) the mean-field phase boundary is reached. Since it is the BKT-type instability which

is expected to be relevant for the phase transition, it is this boundary which must be sought experimentally. Note that the BKT transition preempts the usual [1,4,6,9] prewetting line; however, the latter may now occur on the  $B_1$ - $B_2$  transition boundary.

From Figs. 2–4, we see that the  $t$ - $\nu$  plane phase diagram has the same topology for all three values of  $\rho$  studied. In particular, the two-dimensional BKT-type phase transition occurs for all  $\rho$  values in a finite range of surface interaction potential strengths, with the latter increasing with increasing  $\rho$ . This feature thus appears to be universal.

The reentrant behavior of the uniaxial-biaxial phase transition boundary is, at first, somewhat surprising. Intuitively, one might expect this boundary to shift monotonically to higher  $t$  values with increasing  $\nu$ . However, since the surface free energy contribution (12b) is independent of  $\eta_2$ , the key factor is the  $\nu$  dependence of  $|\eta_2|$  at the phase boundary. For small  $\nu$ ,  $|\eta_2|$  increases with increasing  $\nu$  but, eventually, it will decrease when  $\nu$  is sufficiently large. This is due to the quadratic and higher-order  $|\eta_2|$  terms in (12a), all of which increase  $f$ . The result will be an incremental decrease in the uniaxial-biaxial transition temperature at high  $\nu$  values, yielding reentrant behavior.

Sluckin and Poniewierski [7], in their earlier analysis, considered analytically the special case (in our notation)  $\rho \rightarrow \infty$ . In order to make contact with their result, the (otherwise unphysical) value  $\rho = 10$  was considered by us here (see Fig. 4). Comparing our phase diagram with that in Ref. [7] (the latter for the case of zero external field), we find general agreement. There are only two relatively minor differences: First, Sluckin and Poniewierski find that the first-order transition line between (in our notation) the  $B_1$  and  $B_2$  phases ends in a critical point. As we noted earlier, this is indeed possible on symmetry grounds and, if occurring, would not be found by us due to the nature of the Ritz procedure used. We note that consequently there are at least three possible scenarios—the critical point may be particular to the case  $\rho \rightarrow \infty$ , it may exist only for sufficiently large values of  $\rho$ , or it may exist for all  $\rho$  values. This point still remains open.

Second, Sluckin and Poniewierski suggested alternate possibilities for the location of the BKT line at large  $\nu$  values. We find that the BKT line ends on the bulk phase transition boundary (i.e.,  $t = 1$ ) at the large but finite value of  $\nu$  for all  $\rho$  values. However, since this line is calculated with respect to the Landau theory phase boundary obtained via the Ritz procedure, it is still possible that the BKT boundary is asymptotically parallel to  $t = 1$  for sufficiently large  $\rho$ .

Finally, we note that Sluckin and Poniewierski argued that the qualitative nature of the ( $t$ - $\nu$ ) plane phase diagram should not change when the  $\rho \rightarrow \infty$  constraint is relaxed. This is confirmed by our direct calculation of the phase boundaries (including the BKT transition line) for specific  $\rho$  values.

It is also of interest to compare the results obtained here with those reported for the case of a surface potential *quadratic* in the components of the tensor order parameter [13]. In that case, the existence of a BKT phase

boundary was also predicted. However, the details are different. For the case of a surface interaction potential *linear* in the order parameter, the transition (as found by us here) is necessarily between two ordered states. That is, the surface interaction is analogous to a local external field and always (i.e., at all temperatures above the bulk ordering temperature) leads to ordering in a surface layer. Thus the BKT transition is between two ordered surface states, a higher-temperature one characterized by uniaxial order and a lower-temperature one with biaxial ordering.

For the case of quadratic coupling, on the other hand, the situation is analogous to having a local anisotropy rather than a local applied field. In this case, the higher-temperature phase will be one with complete disorder (both bulk *and* surface) and the BKT transition is to a lower-temperature ordered surface state [13]. However, in both cases, the experimental techniques required to detect a BKT-type phase transition are identical.

Experimentally, one way of observing this phase transition would be using the evanescent-wave ellipsometry technique developed by Chen *et al.* [21]. Here one measures the phase difference  $\Delta$  between  $p$ - and  $s$ -polarized radiation incident at the critical angle and totally reflected from the liquid-crystal–substrate interface. This phase difference is directly proportional to the integrated birefringence at the surface.

In our case, the higher-temperature phase is isotropic in the interface plane and thus nonbirefringent. The lower-temperature (biaxial) state, on the other hand, is birefringent and thus the phase transition should, in principle, be observable by this approach. However, as noted elsewhere [13], the confirmation of the BKT character of this transition by this technique would be difficult as it probes only the singularities associated with static critical behavior, which are very weak for this type of transition.

A much more attractive approach, therefore, is to study the *dynamics* of the critical behavior via inelastic light scattering measurements. Expressions for the scattering intensities to be expected in nematic liquid-crystal systems have been given [13] and can be used to obtain direct experimental confirmation of a BKT-type surface phase transition in such materials.

In summary, we have shown that a new kind of symmetry-breaking surface phase transition is possible in nematic liquid crystals with appropriate boundary conditions. The latter should be attainable in practice and thus the detailed theoretical predictions given here can be tested experimentally. An interesting extension of this work would be to consider the effect of a field applied perpendicular to the boundary on the surface ordering for negative anisotropy materials. For a bulk nematic phase, it is known to result in a tricritical point in the phase diagram [22].

#### ACKNOWLEDGMENTS

This work was supported in part by the National Science Foundation under Science and Technology Center

ALCOM Grant No. DMR89-20147 and the Basic Research Foundation, administered by the Israeli Academy of Arts and Sciences, Jerusalem, Israel. Reciprocal visits by D.W.A. at the Weizmann Institute of

Science and R.M.H. at the Liquid Crystal Institute, Kent State University, greatly facilitated the progress of this work. We acknowledge helpful discussions with E. I. Kats and V. V. Lebedev.

- 
- [1] P. Sheng, *Phys. Rev. Lett.* **37**, 1059 (1976).  
 [2] K. Miyano, *Phys. Rev. Lett.* **43**, 51 (1979).  
 [3] D. W. Allender, G. L. Henderson, and D. L. Johnson, *Phys. Rev. A* **24**, 1086 (1981).  
 [4] P. Sheng, *Phys. Rev. A* **26**, 1610 (1982).  
 [5] M. M. Telo da Gama, *Mol. Phys.* **52**, 611 (1984); A. Poniewierski and T. J. Sluckin, *Mol. Cryst. Liq. Cryst.* **111**, 373 (1984).  
 [6] A. Mauger, G. Zribi, D. L. Mills, and John Toner, *Phys. Rev. Lett.* **53**, 2485 (1984).  
 [7] T. J. Sluckin and A. Poniewierski, *Phys. Rev. Lett.* **55**, 2907 (1985); and in *Fluid Interfacial Phenomena*, edited by C. A. Croxton (Wiley, New York, 1985), Chap. 5; see also P. Sheng, B.-Z. Li, M. Zhou, T. Moses, and Y. R. Shen, *Phys. Rev. A* **46**, 946 (1992).  
 [8] A. K. Sen and D. E. Sullivan, *Phys. Rev. A* **35**, 1391 (1987).  
 [9] H. Nakanishi and M. E. Fisher, *Phys. Rev. Lett.* **49**, 1565 (1982); see also M. Schick, *Phys. Rev. Lett.* **54**, 2169 (1985).  
 [10] D. E. Sullivan and M. M. Telo da Gama, in *Fluid Interfacial Phenomena*, edited by C. A. Croxton (Wiley, New York, 1985), Chap. 2.  
 [11] V. L. Berezinskii, *Zh. Eksp. Teor. Fiz.* **61**, 1144 (1971) [*Sov. Phys. JETP* **34**, 610 (1971)].  
 [12] J. M. Kosterlitz and D. J. Thouless, *J. Phys. C* **6**, 1181 (1973).  
 [13] R. M. Hornreich, E. I. Kats, and V. V. Lebedev, *Phys. Rev. A* **46**, 4935 (1992).  
 [14] R. M. Hornreich and S. Shtrikman, *Mol. Cryst. Liq. Cryst.* **165**, 183 (1988).  
 [15] That is, we regard the system as symmetric about  $\zeta=0$  with the surface interaction existing in an infinitesimal region centered about this point (see, e.g., Refs. [6,12]. Alternate definitions are possible, they effect only the connection between  $\nu$  and the physical surface interaction potential.  
 [16] D. L. Stein, *Phys. Rev. B* **18**, 2397 (1978).  
 [17] H. J. Coles, *Mol. Cryst. Liq. Cryst.* **49**, 67 (1978).  
 [18] Hiroshi Yokoyama, *J. Chem. Soc. Faraday Trans. 2* **84**, 1023 (1988).  
 [19] Yokoyama presents his results in terms of  $g=4.0$  and  $0.09$ , respectively, where  $g$  is defined in Ref. [4], and is equivalent to  $G=38$  and  $0.85$  erg/cm<sup>2</sup>.  
 [20] H. Yokoyama, *Mol. Cryst. Liq. Cryst.* **165**, 265 (1988).  
 [21] W. Chen, L. J. Martinez-Miranda, H. Hsiung, and Y. R. Shen, *Phys. Rev. Lett.* **62**, 1860 (1989).  
 [22] P. Fan and M. J. Stephen, *Phys. Rev. Lett.* **25**, 500 (1970).